Control Structure Synthesis for Operational Optimization of Mixed Refrigerant Processes for Liquefied Natural Gas Plant

Yuli Amalia Husnil and Moonyong Lee
School of Chemical Engineering, Yeungnam University, Dae-dong, Kyeongsan 214-1, Korea

DOI 10.1002/aic.14430
Published online March 11, 2014 in Wiley Online Library (wileyonlinelibrary.com)

The best control structures for the energy optimizing control of propane precooled mixed refrigerant (C_3MR) processes were examined. A first principles-based rigorous dynamic model was developed to analyze the steady-state and dynamic behaviors of the C_3MR process. The steady-state optimality of the C_3MR process was then examined in a whole operation space for exploring the feasibility of the energy optimizing control for possible control structures. As a result, the temperature difference (TD) between the warm-end inlet and outlet MR streams was exploited as a promising controlled variable to automatically keep the liquefaction process close to its optimum. The closed-loop responses were finally evaluated for every possible control structure candidate. Based on the steady-state optimality and the dynamic performance evaluation, several control structures with a TD loop were proposed to be most favorable for the energy optimizing control of the C_3MR process. The proposed optimality approach can be applied to any natural gas liquefaction process for determining a proper controlled variable for optimizing operation. © 2014 American Institute of Chemical Engineers
AIChE J, 60: 2428–2441, 2014

Keywords: liquefied natural gas process control, energy optimizing control, control structure synthesis, mixed refrigerant process, natural gas liquefaction process, cryogenic exchanger, rigorous dynamic simulation

Introduction

Natural gas (NG) is a promising source of clean energy with its clean burning characteristics. Recent boom of shale gas has further spotlighted NG as an increasingly important source of energy. The steadily increasing world energy demand has prompted the rapid growth of liquefied natural gas (LNG) production.[1] Mixed refrigerant (MR) systems dominate in liquefaction processes in the LNG industry. The propane precooled mixed refrigerant (C_3MR) cycle is the leading technology used by approximately 90% of onshore LNG plants. The use of a MR allows the refrigerant to boil over a temperature range, which results in high efficiency liquefaction.[2]

The research trend regarding the MR process is to determine its optimal design and operation. Hatcher et al.[3] tested eight objective functions to discover the most appropriate for improving the efficiency of the C_3MR process. Wang et al.[4] proposed a new mathematical program for LNG liquefaction operational optimization using C_3MR as the process. Helgestad[5] also contributed to modeling and optimizing the C_3MR process using the potential degree of freedom approach. In a more general case, many studies have examined the optimization of other MR NG liquefaction technologies.[6–8]

Most optimization studies focused on designing a process with higher energy efficiency. Conversely, a very few studies have addressed the optimality of the liquefaction process in a process control perspective.[9] Stable and economic operation of the C_3MR process is still challenging due to its complicated steady-state and dynamic behaviors from its intensified process configuration. A plant frequently encounters disturbances that disrupt the performance of the plant, that is, operation stability and product quality. The action of controllers on bringing back controlled variables to their set points can be energy consuming, which violates the purpose of optimization. Therefore, a plant should be equipped with at least one control loop with the specific purpose of controlling the energy efficiency during plant operation. This is related to the idea of a self-optimizing control structure that can achieve optimal adjustment of the manipulated variable by controlling a single variable.[10]

The main aim of this study was to develop the control structures for operational optimization of the C_3MR process and stable operation as well. The steady-state optimality behavior was analyzed through the whole space of the main operation variables to explore the optimality of the possible control structures. The feasibility of a temperature difference (TD) control loop was exploited as one of the approaches to remain or maximize the energy efficiency of the process. The control structures were classified into a fixed and floating LNG production case. Six possible basic control structures were considered with several other derivative structures examined. Several tests were conducted to locate the major source of the disturbances as well as to gain an understanding of interactions that occur among variables in the C_3MR process. The results from an analysis of the interaction measure and the information obtained from the disturbance tests were compared and analyzed to support the selection of the

Correspondence concerning this article should be addressed to M. Lee at mynlee@yu.ac.kr.

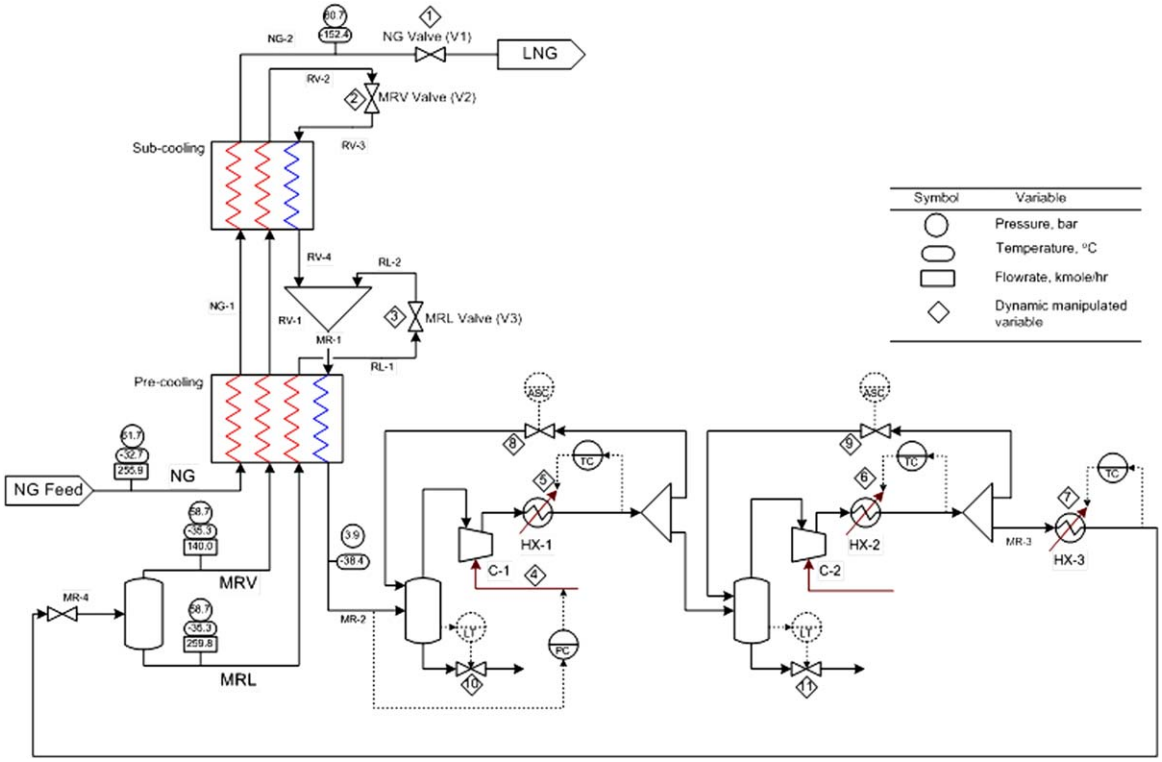

Figure 1. The flow sheet and DOF of C_3MR liquefaction cycle.

[Color figure can be viewed in the online issue, which is available at wileyonlinelibrary.com.]

best control structure. The dynamic response of the LNG temperature and the required compressor duty were the final criteria used to assess the performance of each structure.

The steady-state optimality analysis proposed in this study is expected to add useful insights on the operational behavior of the C_3MR process particularly. Nevertheless, this approach can also be applied for other NG liquefaction processes.

Process Description

Figure 1 shows the C_3MR liquefaction process. The cryogenic exchanger in the liquefaction unit was divided into two parts, precooling and subcooling. The MR cycle has two compressor stages and two after-coolers. Propane refrigeration was not modeled rigorously in this study, and is simply represented as a cooler at the end of the compressor assembly (HX-3). NG enters the precooling section at 61.7 bar and -32.7°C, where it is cooled and liquefied (NG-1). In the second section of the exchanger, the LNG was subcooled to -152.4°C (NG-2) before it entered the next treatment. The NG feed for the liquefaction process in this study was assumed to be already precooled in propane refrigeration.

Before entering the precooling section, the MR was flashed to two separate warm-end streams as a mixed refrigerant vapor (MRV) and mixed refrigerant liquid (MRL). Similar to NG, the MRV was cooled and liquefied (RV-1), whereas the MRL was subcooled (RL-1). The MRV from the precooling section was then subcooled in the next section (RV-2) before being expanded to a low pressure through the MRV valve. This expansion led to a small decrease in temperature and formed a small amount of vapor (RV-3). This cold MRV provided the cooling duty for subcooling the LNG and the incoming MRV. The partially vaporized MRV (RV-4) was then remixed with the expanded MRL (RL-2) and acts as a cold stream (MR-1) that exchanges heat with three hot streams in the precooling section. The warm-end outlet stream (MR-2) of the cold refrigerant that exits the exchanger as a low pressure gas experiences two stages of compression and cooling (MR-3) before being condensed in propane refrigeration (MR-4).

In this study, the process simulator HYSYS^{TM} was used for a rigorous dynamic simulation of the C_3MR process. The Peng–Robinson equation of state supporting the widest range of operating conditions and the largest variety of systems were used to predict the simulated vapor–liquid equilibrium. Table 1 lists the steady-state values of the main variables used in this study as a base case.

Degrees of Freedom

The number of actual degrees of freedom (DOF), (N_{ss}), can be calculated by subtracting the number of DOF without steady-state effect, (N_0), from the number of dynamic manipulated variables, (N_{MV}).[11] Hence, $N_{ss} = N_{MV} - N_0$. The C_3MR liquefaction cycle used in this study has 11 N_{MV} as follows:

a. One NG feed valve (1)
b. Two choke valves for the MR cycle (2) and (3)
c. One common speed variable for the MR compressors (4)
d. Flow of cooling medium for the MR compressor coolers (5) and (6)
e. Flow of cooling medium in the propane precooled MR cooler (7)
f. Two spillback valves (8) and (9)
g. Two release valves of knock-out drums (10) and (11)

No liquid level needs to be controlled in the recycle loop ($N_0 = 0$), so $N_{ss} = 11$.

In the MR compression unit, there are four variables that need to be tightly controlled: the compressor suction

Table 1. Steady-State Values of State Variables in the Base Case

NG Stream		MR Stream	
Source pressure (bar)	61.7	Suction pressure(bar)	3.9
Sink pressure (bar)	60.7	Suction temperature (°C)	−52.1
Source temperature (°C)	−32.7	Temperature after propane refrigeration(°C)	−32.9
LNG temperature (°C)	−152.4	temperature difference between the warm-end inlet and outlet MR streams (°C)	17.0
Flow rate (kmol/h)	255.8	MRL flow rate (kmol/h)	289.0
		MRV flow rate (kmol/h)	124.6
Composition (Mole Fraction)		Composition (Mole Fraction)	
Nitrogen	0.0498	Nitrogen	0.0602
Methane	0.8706	Methane	0.4759
Ethane	0.0507	Ethane	0.3345
Propane	0.0198	Propane	0.1293
i-Butane	0.0044	*i*-Butane	–
n-Butane	0.0045	*n*-Butane	–
i-Pentane	0.0001	*i*-Pentane	–
n-Pentane	0.0001	*n*-Pentane	–

pressure, outlet temperatures from the two after-coolers, and outlet temperature from propane precooled unit. Variables (4), (5), (6), and (7) were assigned preferentially to manipulate these four controlled variables, as shown in Figure 1. By controlling those variables, the liquefaction unit was isolated from the potential problems caused by pressure and temperature variations in the compressor and propane precooled units. Therefore, the observed phenomena are mostly the real behavior from the liquefaction unit itself. In addition, the spillback valves, which are commonly used as the control element for an antisurge controller, remain closed during normal operation. Similarly, the two release valves in the knock-out drums are also normally kept closed because the feed to compressor is normally in the gaseous phase.

Consequently, there are only three DOF that can be used to achieve the control objectives. Those DOF are the NG, MRV, and MRL flows.

Control Objectives

The main operation objective in any type of NG liquefaction processes is to produce LNG with a prespecified temperature in a stable and economic manner under operation constraints. Control of the LNG product temperature is essential and takes precedence over other control tasks. Conversely, the LNG production rate can be either a controlled or manipulated variable depending on the control and operation principles of the process concerned. Therefore, basic regulatory control problems can be classified into two categories depending on the role or circumstances of the LNG product stream: (1) the LNG production rate is determined or fixed by the factors such as production planning and control of the upstream variables that are not associated with liquefaction control (a fixed production case); and (2) the LNG production rate is available to be used for liquefaction control as a manipulated variable (a floating production case). Both cases have extra DOF of 1 and 2, respectively. The remaining extra DOF can be used for other purposes to improve the liquefaction efficiency and/or stable operation. These two regulatory control cases were considered in relation to the optimizing control task.

Auxiliary Controlled Variable for Operational Optimization

This section briefly discusses the several variables with potential use in operational optimization or self-optimizing control of the C_3MR liquefaction process. One of the main issues in C_3MR process control is to determine the correct variable for optimal operation of the liquefaction process. A self-optimizing controlled variable[10] in the C_3MR liquefaction process is a variable that can always keep the process operation at a minimal MR compressor duty when it is remained constant. The variables considered were the MRL or MRV flow rate, MRL/MRV or MRV/MRL flow rate ratio, and TD between the warm-end inlet and outlet MR streams.

The MRL or MRV flow rate has the potential to be a self-optimizing controlled variable because the movement of each respective control valve will affect the suction pressure and compressor speed. The MRL/MRV or MRV/MRL ratio can also be a candidate because maintaining the refrigerant to always have an appropriate mixture of high and low boiling point components results in a high specific refrigeration effect at a relatively low refrigeration temperature.[12] In a simple refrigeration cycle, the difference between the condensation and evaporation temperature is considered the dominant factor in the relationship between heat transfer and compressor work.[13] Operating the refrigeration cycle at a constant TD might maintain the overall efficiency of the cycle. In the C_3MR liquefaction process, the TD is referred to as the TD between the warm-end inlet (either MRV or MRL in Figure 1) and outlet (MR-2 in Figure 1) MR streams. The effect of keeping constant each of the previously mentioned variables onto the energy demand of the process was analyzed through a steady-state optimality map in the operation space, as will be shown in Figure 3A.

From a design point of view, the efficiency of heat transfer in a cryogenic exchanger is commonly associated with a minimum internal temperature approach (MITA). This variable is used widely as a constraint for the design optimization of a cryogenic exchanger that should be kept as low as possible because a larger MITA means that more energy needs to be transferred to the process through the compressor.[14] Based on this, the efficient process that results from design optimization is still expected to be preserved on the real plant operation if the MITA value is maintained by a particular control loop. The MITA and TD are closely related, as shown in Figure 2B: the MITA value tends to increase with increasing TD. Therefore, for a given NG feed condition, the MITA would be maintained automatically by controlling TD, whereas the MITA cannot be measured directly online. Conversely, having the same TD value does not lead to the same MITA for different feed conditions. As

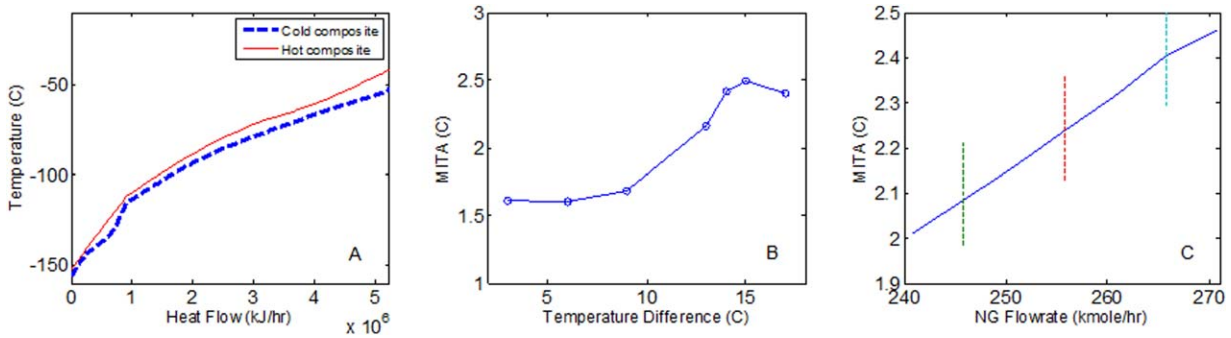

Figure 2. (A) Composite curve of the C_3MR liquefaction process, (B) correlation between the TD and MITA, and (C) correlation between the NG flow rate and MITA.

[Color figure can be viewed in the online issue, which is available at wileyonlinelibrary.com.]

shown in Figure 2C, at a constant TD, the MITA value increased with increasing NG flow rate (solid line). The MITA also changed when the NG feed conditions, such as pressure, temperature, and composition, were disturbed at a constant NG flow rate (dashed vertical line).

Steady-State Optimality Behavior of the C_3MR Liquefaction Process

The LNG temperature is a complex function of every state variable associated with the liquefaction process. For a given NG feed, there are an infinite number of steady-state solution sets in the NG, MRV, and MRL flow rate to meet a specified LNG temperature. Because each solution set results in different liquefaction efficiency, it is important to find the optimum solution set and operate the liquefaction process at the optimum operation point. Figure 3A shows the steady-state optimality map for a given LNG temperature (−152.4°C). An optimality map was composed by fixing the NG feed pressure, temperature, and composition as well as the compressor suction pressure and separator temperature with the base case values listed in Table 1. In the map, the dashed, dotted, and three-layered lines represent the constant MRV flow rate, MRL/MRV flow ratio, and TD lines, respectively. The "star" point represents the base operating conditions of the C_3MR process. One can see that this point is crossed by the four constant lines that denote the operating conditions in the particular point. By putting an arbitrary point on the map the complete operating conditions can be obtained. As seen from the map, larger NG flows require larger MRL (or MRV) flows and compressor duties to maintain the same LNG temperature. A larger NG flow results in a smaller TD at a constant MRL flow but a larger TD was observed at a constant MRV flow.

The map also shows that for each NG flow rate, there is an optimum point to give a minimum compressor duty: the MRV flow rate decreases with increasing MRL flow rate (i.e., the MRL/MRV ratio increases) to achieve the same LNG temperature, and the required compressor duty

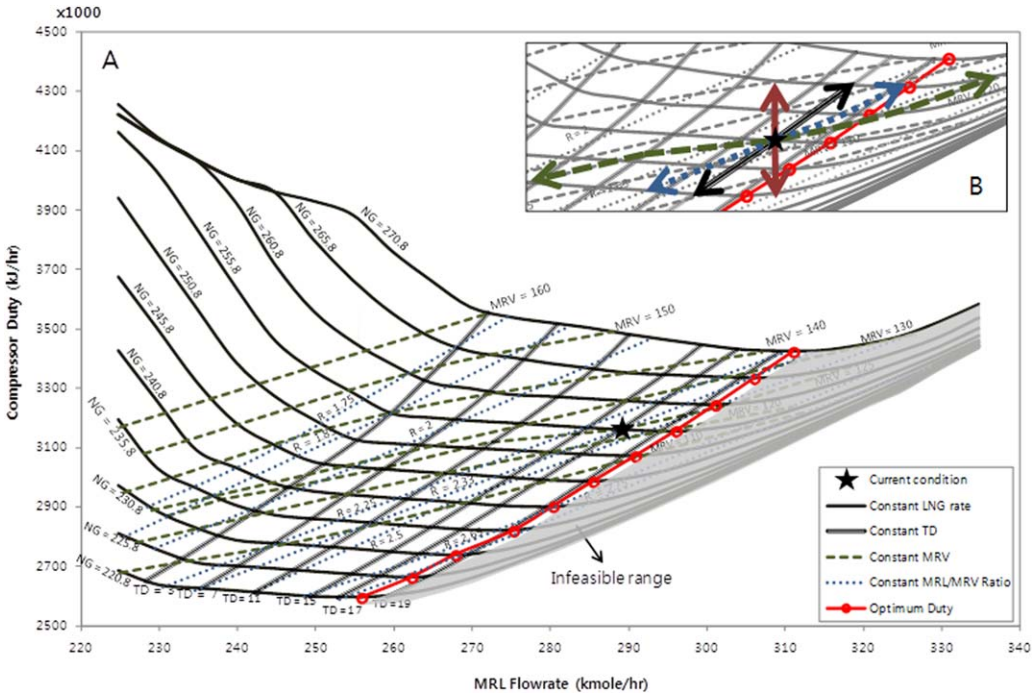

Figure 3. Steady-state optimality map of the C_3MR liquefaction process for a given LNG temperature (−152.4°C).

[Color figure can be viewed in the online issue, which is available at wileyonlinelibrary.com.]

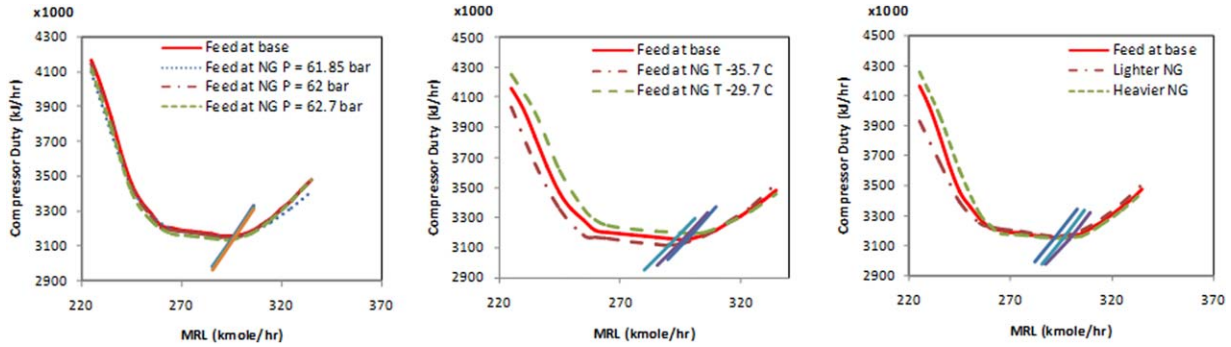

Figure 4. Steady-state operational curve at different feed conditions.

[Color figure can be viewed in the online issue, which is available at wileyonlinelibrary.com.]

decreases. Conversely, the required compressor duty increases after an optimum MRL flow rate. The circled-solid line in the map denotes the minimum compressor duty trajectory that connects the optimum points for different NG flow rates. In addition, the optimum for the minimum compressor duty occurs at the dew temperature of the warm-end outlet MR stream (MR-2), which means the MR stream (MR-2) is on its dew temperature at every point on the optimum duty trajectory. In a real operation, operating a compressor with a feed stream above the dew point temperature is strictly avoided because it can damage the compressor blade if the feed contains some drops of liquid. Therefore, the optimum duty line divides the operation map into feasible and infeasible regions: the right side of the optimal line indicates an infeasible operation region.

The existence of an optimum operation point giving a minimum compressor duty can be explained as follows. A decrease in the MRV flow rate means that the opening percentage of its corresponding valve is reduced, which will result in a lower suction pressure. To increase it back to its set point, the MR compressor will be operating at a lower speed and the required duty will also decrease. The correlation between the MRV flow rate and compressor duty is true only when the control loop that connects the suction pressure and compressor speed is closed. In an infeasible operation region, because the temperature of the MR exceeds the dew point temperature, the warm-end MR stream (MR-2) carries some liquid, which in turn will be sent to knock-out drum while the vapor proceeds to the compressor. Consequently, it decreases the MR available to the refrigeration cycle. The compressor will increase its speed to meet the amount of refrigerant required to maintain the LNG temperature at its set point, resulting in an increase in compressor duty. This process will also suffer from MR loss because the process has no scheme to draw out the liquid MR from the knock-out drum and feed it back to the MR cycle.

When the temperature of the separator (or the warm-end inlet MR stream) is fixed, a constant TD means that the temperature of the warm-end outlet MR stream is constant. Figure 3A shows that the optimum trajectory moves gradually from outside TD = 19°C to close to TD = 17°C. This suggests that as the operation moves to the lower part of the map in Figure 3A, the MR begins to condense at higher temperature. The dew point temperature of a mixture is pressure and composition dependent. In this process, the suction pressure is fixed tightly. Hence, the dew point temperature is affected solely by the composition of the MR on that stream. As the operation moves closer to the lower part of the minimum duty trajectory, the MRL/MRV ratio is higher, which results in a heavier refrigerant circulating in the MR cycle and a higher dew temperature. Regardless of its gradual increase with increasing NG flow, the dew temperature trajectory (or the minimum duty trajectory) still coincides reasonably with the constant TD line, in this particular case, TD = 19°C. Furthermore, most constant TD lines are parallel to most parts of the minimum duty trajectory.

Operating the cryogenic exchanger at the optimum line is not recommended. A small variation in either MRL or MRV flow rate will quickly move the process to the infeasible area. Although the process is equipped with excellent performance control structures, the loss that can occur during the transient period, even it is very small, must also be considered. Therefore, although the maximum efficiency of the process can be obtained when the process is operated on this optimum line, in practice, to secure some safety margin in the compressor operation, the process should be operated a

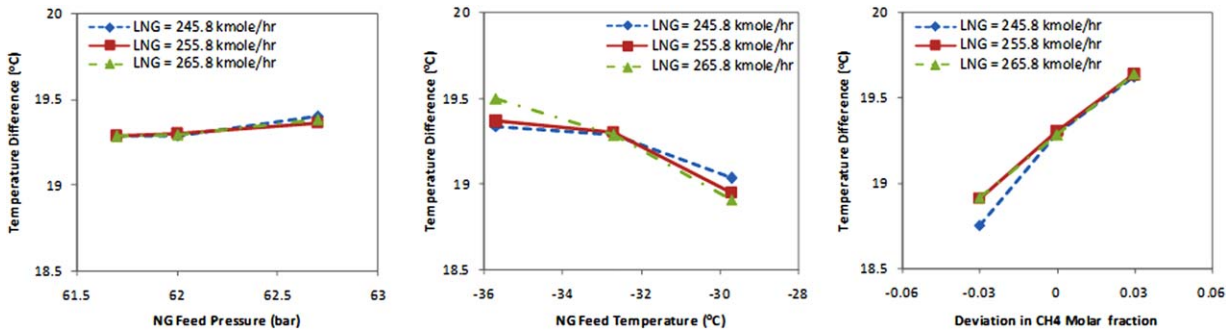

Figure 5. How the optimum TD is shifted when the NG feed condition is changed.

[Color figure can be viewed in the online issue, which is available at wileyonlinelibrary.com.]

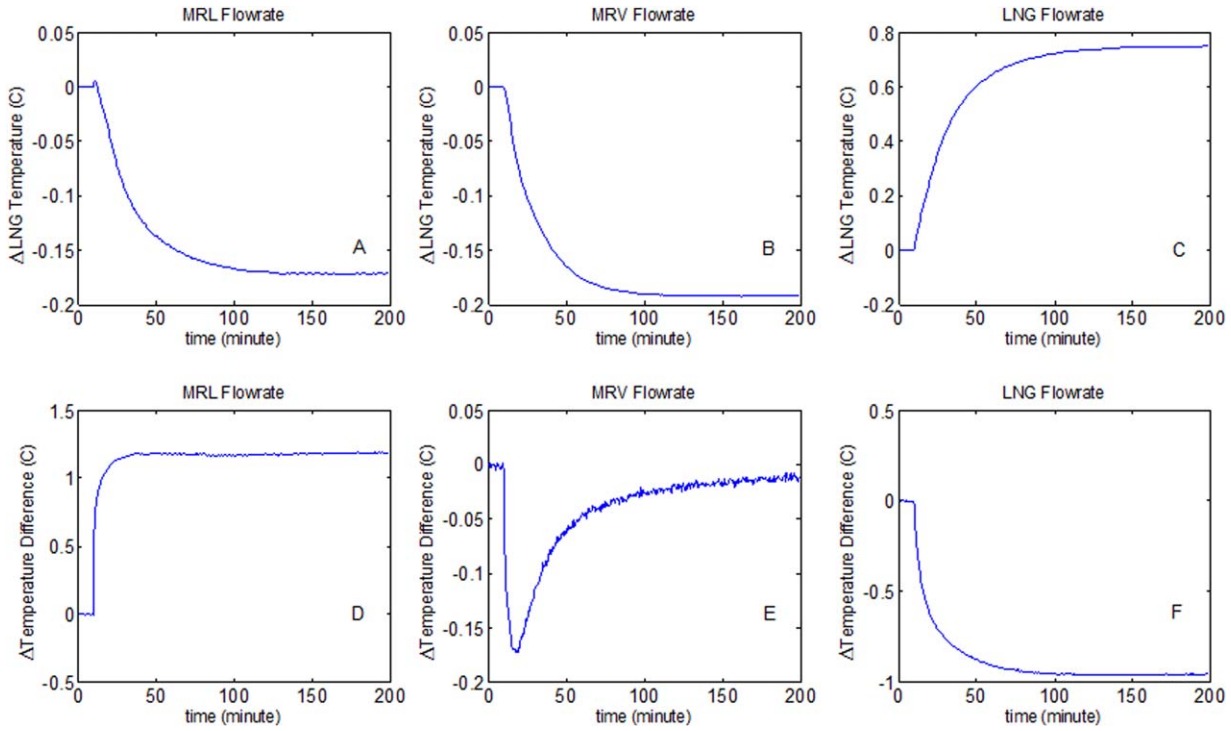

Figure 6. Responses of the controlled variables after increasing the set point of the MRL, MRV, and NG flow rate.

[Color figure can be viewed in the online issue, which is available at wileyonlinelibrary.com.]

little bit away from this ideal optimum duty point, that is, the temperature of the warm-end MR outlet stream needs to be somewhat higher than its dew temperature. In this study, the base case TD was chosen arbitrarily as 17°C for a NG flow rate of 255.8 kmol/h so that the process has a proper safety margin but still operates near the optimum.

The steady-state optimality map also provides useful insight into the steady-state behavior of the possible control structures. Figure 3B magnifies the region of the current condition to show an example of the possible trajectories that this process will follow when the NG flow rate is increased or decreased from the normal operating conditions. This flow rate variation was carried out using four different scenarios: constant MRL (solid line), constant MRV (dashed line), constant TD (three-layered line), and constant MRL/MRV ratio (dotted line). Figure 3B shows that increasing or decreasing the NG flow rate at a constant MRL flow rate, MRV flow rate, and MRL/MRV ratio will drift the liquefaction process either quickly away from the optimum point or cross the dew point line to reach the infeasible region. This means that any control structure using these variables as a controlled variable will suffer from this problem for the NG feed flow variation. Only by following the constant TD line can the process always be kept within a feasible region with a constant safety margin. Compared to the constant MRV and constant MRL/MRV ratio line, the constant TD lines are parallel to most parts of the optimum trajectory, where each point in these lines has an almost equal distance to the respective optimum point. This observation suggests that the TD can be a promising controlled variable for optimizing operation of the C_3MR liquefaction process. This distance was adapted to the term process liquefaction efficiency, η, defined by Eq. 1

$$\eta = 1 - \frac{Q_i - Q\mathrm{opt}_i}{Q_i} \tag{1}$$

where notation, i, corresponds to a point in the constant NG flow rate line.

Making the process to follow, this constant TD line can maintain the process liquefaction efficiency given in Eq. 1. For example, at every point in the line of TD = 17°C, the process will maintain 99% efficiency within a feasible region under NG flow rate variations. This analysis shows that a control structure keeping a constant TD can be more beneficial than other structures keeping any of the other three variables, such as the MRV, MRL, and MRL/MRV ratio because it prevents the process from losing either safety margin or energy efficiency for the NG feed flow variation. This suggests that the TD is a promising candidate as a controlled variable to achieve self-optimizing control for the C_3MR liquefaction process.

The optimal TD can be changed for different feed conditions because the steady-state optimality is also a function of the NG feed pressure, temperature, and composition. Accordingly the set point of the TD also might need to be reassigned depending on the extent of the changes in the feed conditions. Figure 4 shows how a constant NG flow line (i.e., the compressor duty line) and the minimum duty trajectory are affected by variations in the feed conditions. For feed composition variations, the molar fraction of CH_4 was increased by 0.015 with a concomitant decrease in the molar fraction of C_2H_6. As shown in the figure, the position and shape of the constant NG flow line and the minimum duty trajectory were not changed sensitively for the assumed range of feed variations. Figure 5 shows how the optimal TD values are shifted by changes in the feed condition. As shown in the figure, the optimum TD tends to increase with

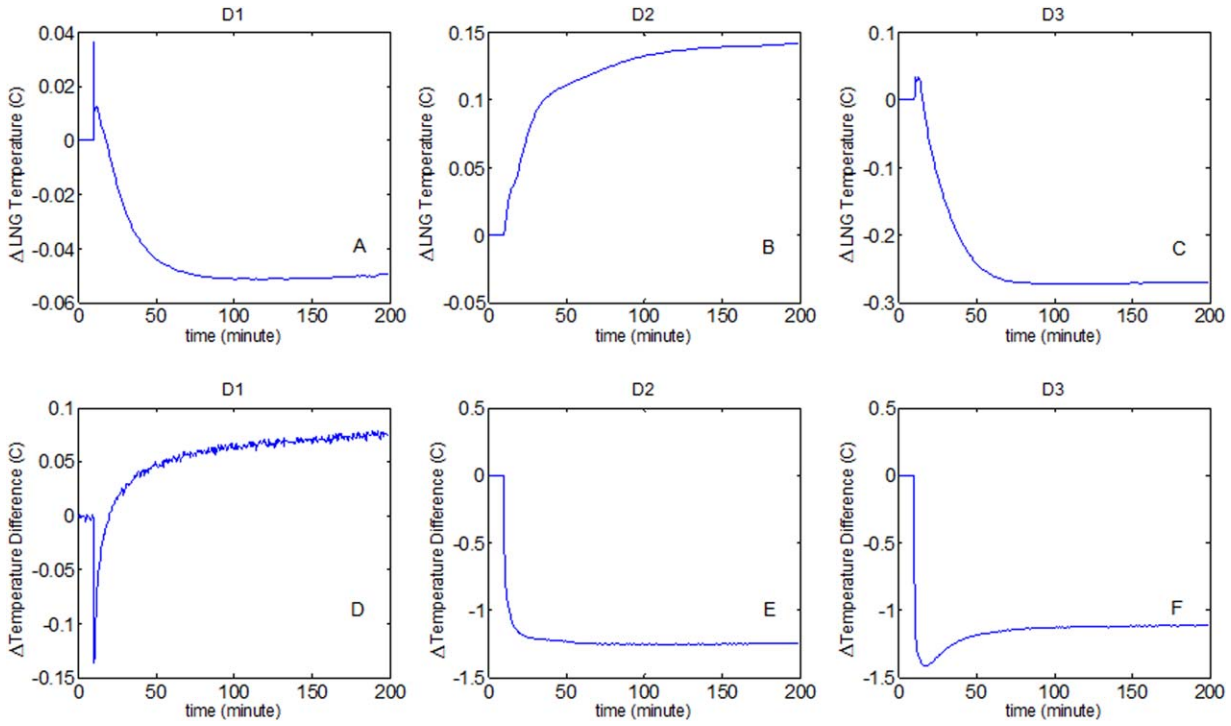

Figure 7. Responses of the controlled variables after D1, D2, and D3 when all flow rates were controlled.

[Color figure can be viewed in the online issue, which is available at wileyonlinelibrary.com.]

increasing feed pressure and CH_4 fraction and decreasing feed temperature but its variation was not significant for the assumed range of feed variations.

Open-Loop Dynamic Behavior

The C_3MR liquefaction cycle consists of subsystems that are connected to several parallel paths in a cryogenic heat exchanger. In this type of system, an input will affect not only one output but also several physical properties in different subsystems.[15] This section includes several tests to locate the major source of the disturbances as well as to gain an understanding of interactions that occur among variables in the C_3MR process.

Variations in the mass balance

To examine the effects of changes in the mass balance associated with the main manipulated variables, a 1% step increase was introduced at 10 min for the NG, MRV, and MRL flow. When the step change was made in the flow rate of a single variable, the flow rates of the other two manipulated variables were maintained tightly by the corresponding flow controllers under all other controlled variables associated with the compressor and propane precooled units also being controlled tightly. Figure 6 shows the responses of the main controlled variables by this flow rate variation.

As shown in the figure, increasing either the MRV or MRL flow rate increases the driving force of heat transfer between the NG stream and cold refrigerant, which leads to a temperature decrease in the LNG stream. In particular, for an increase in the MRL flow rate, the cryogenic heat exchanger will have more capacity for liquefaction, as indicated by the higher TD.

An increase in MRV flow does not produce the same response in the TD as when the MRL flow increases. As the MRV flow increases, more heat is transferred to the cold refrigerant in the precooling section. Therefore, MR-2 temperature increases and the TD decrease. As shown in Figure 6E, the TD response by a change in the MRV flow showed severe undershoot, which suggests the poor performance of TD-MRV pairing. This undershoot indicates that the system consists of two different dynamics that occur after the MRV flow rate set point is increased. In the first path, as the MRV flow rate is increased with the others held constant, more heat is transferred to a cold refrigerant. Therefore, temperature of the warm-end outlet MR stream increases and the TD decreases with a constant MR inlet temperature. In the second path, the cold energy will be then available in excessive amounts when the MRV stream returns from the subcooling exchanger and is mixed with the MRL flow. The temperature of the warm-end outlet MR then decreased, resulting in an increase in TD.

Adding more NG to the process will obviously increase the heat load in both precooling, which results in a decrease in TD, and the subcooling section, which consequently increases the LNG temperature. The distinctly rapid response of the TD by MRL or NG manipulations and the relatively slow response of the LNG temperature by MRV or NG manipulated variables suggests that structures, such as the (T-MRV, TD-MRL), (T-MRV, TD-NG), and (T-NG, TD-

Table 2. List of the Manipulated and Controlled Variables

Manipulated Variable	Controlled Variable	Configuration	Possible Pairings
NG	T	(NG, MRV)	(T-NG, TD-MRV)
MRV	TD		(T-MRV, TD-NG)
MRL		(MRV, MRL)	(T-MRV, TD-MRL)
			(T-MRL, TD-MRV)
		(NG, MRL)	(T-NG, TD-MRL)
			(T-MRL, TD-NG)

Table 3. Results from RGA Analysis

	(NG, MRV)		(MRV, MRL)		(NG, MRL)	
	NG	MRV	MRV	MRL	NG	MRL
T	0.042	**0.958**	**0.992**	0.008	**1.222**	−0.222
TD	**0.958**	0.042	0.008	**0.992**	−0.222	**1.222**

The bold characters are to show that those numbers are the closest to 1.

MRL), probably results in natural implicit decoupling because of the significantly different response speed. Note that throughout this article, T denotes the LNG temperature.

Variation in NG feed condition

The NG feed pressure (D1), temperature (D2), and composition (D3) were varied as the main disturbances that are expected to propagate to the C_3MR liquefaction process. The value of the deviation for each variable was chosen arbitrarily but still remained in the linear range. The NG inlet pressure and temperature were increased by 0.15 bar and 1.5°C, respectively. In the case of disturbances associated with the NG feed composition, the mole fraction of methane and ethane were varied by 0.015 downward and upward, respectively. These tests were conducted by fixing the flow rate of all the manipulated variables.

Figure 7 presents the responses of the LNG temperature (T) and TD after a step change in D1, D2, and D3. The step change in NG pressure causes a temporary hunting of NG flow, which results in an initial inverse response. Conversely, a higher NG pressure eventually requires less cold energy to be liquefied and subcooled due to its lower enthalpy of condensation, and finally decreases the LNG temperature and increases the liquefaction capacity of the cryogenic exchanger. A heavier NG has higher heat content and will transfer more heat to the cold refrigerant, resulting in a decrease in TD. Conversely, higher ethane content promotes the liquefaction of NG with the respective composition. Therefore, at a constant NG flow rate, the same total amount of MR will produce LNG with a lower temperature.

Interaction Analysis

The C_3MR system examined in this study is a nonsquare system with two controlled variables and three manipulated variables. Six possible control structures were examined by squaring it down to a 2 × 2 system. Table 2 lists the manipulated and controlled variables for the C_3MR liquefaction cycle along with possible pairings. The third column in Table 2 lists the possible configurations which characterized by the manipulated variables that are used for controlling the controlled variables. For instance, (NG, MRV) denotes a control structure where the NG and MRV flow rate are the manipulated variables. The fourth column of the table lists possible pairings in one particular configuration.

Steady-state and dynamic-state interaction analyses were carried out to gain insight into the loop interactions of the control structures. This knowledge is useful supporting evidence for gaining a thorough understanding of the C_3MR liquefaction process. Two popular methods were used to analyze the interaction between variable pairings: RGA (Relative Gain Array) and DRGA (Dynamic Relative Gain Array).

RGA can be used to analyze the steady-state interactions between the control loops and mainly to screen out the undesirable pairing alternatives. Table 3 presents the results of RGA analysis. RGA analysis suggests (T-MRV, TD-NG), (T-MRV, TD-MRL), and (T-NG, TD-MRL) pairings, which indicates no significant steady-state interaction from their RGA element values close to 1.

Despite its usefulness in providing a general view of the interactions among the variables, RGA is based on the static gains that neglect the dynamics of the process. Dynamic RGA[16] is a useful tool for measuring the interactions of multivariable processes, which have a broader view on the dynamic behavior compared to RGA. DRGA of possible pairings was calculated based on the transfer function matrix shown in Eq. 2, which was obtained from a step test in a rigorous dynamic simulation

$$\begin{bmatrix} T \\ TD \end{bmatrix} = \begin{bmatrix} \dfrac{0.295}{(2.423s+1)(27.96s+1)(27.817s+1)} & \dfrac{-0.154}{(20.527s+1)(0.001s+1)(0.001s+1)} & \dfrac{-0.059}{(1.138s+1)(22.886s+1)(0.001s+1)} \\ \dfrac{-0.374}{-(3.685s+1)(143.72s+1)(24.885s+1)} & \dfrac{-0.008(-323.92s+1)}{(25.68s+1)(2.612s+1)(0.047s+1)} & \dfrac{0.409}{(6.174s+1)(0.065s+1)(0.382s+1)} \end{bmatrix} \begin{bmatrix} NG \\ MRV \\ MRL \end{bmatrix} \tag{2}$$

DRGA analysis confirmed the results from RGA analysis for the (MRV, MRL) and (NG, MRL) configurations (Figure 8). For the (NG, MRV) configuration, however, the recommended pairing by the DRGA was changed from off-diagonal to its reverse at the high frequency range.

Dynamic Response Evaluation

The results from interaction measure analyses can show a general view of the interactions in control pairings, but not sufficient for deciding the final control scenario that best fits the C_3MR process. A rigorous evaluation based on a dynamic response test is essential for each pairing combination to determine the best control structure. The arrangement of the control structure for the C_3MR process can be classified into two cases: (1) a fixed LNG production case, where the LNG flow is determined or fixed by other factors not associated with liquefaction control; and (2) a floating LNG production case, where the LNG flow rate can be used as a manipulated variable for liquefaction control. Thus, configurations listed in Table 2 can be classified as follows. The (MRV, MRL) configuration belongs to the fixed production

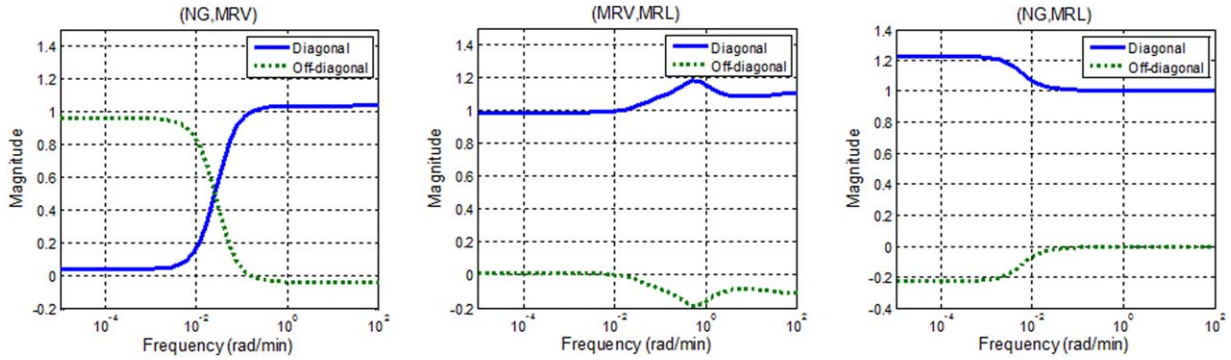

Figure 8. DRGA plots.

[Color figure can be viewed in the online issue, which is available at wileyonlinelibrary.com.]

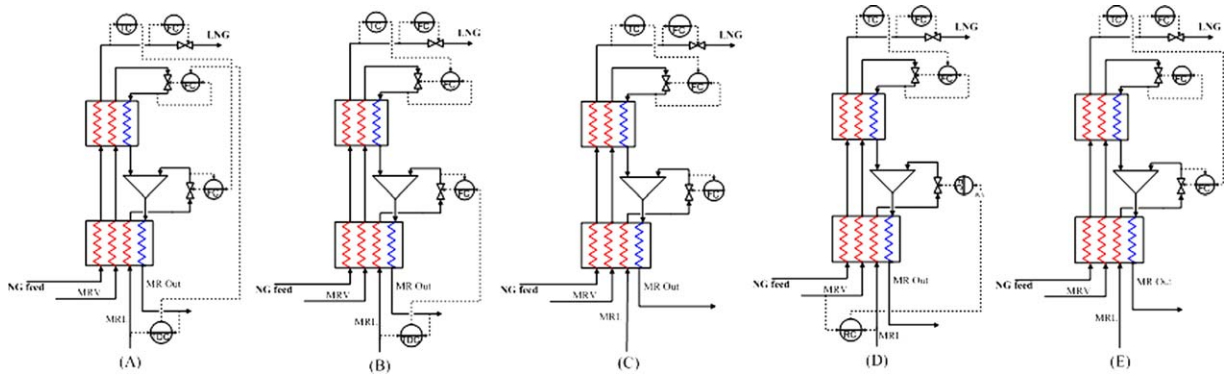

Figure 9. Arrangement for (A) (T-MRL, TD-MRV), (B) (T-MRV, TD-MRL), (C) (T-MRV, fixed-MRL), (D) (T-MRV, ratio-MRL), and (E) (T-MRL, fixed-MRV).

[Color figure can be viewed in the online issue, which is available at wileyonlinelibrary.com.]

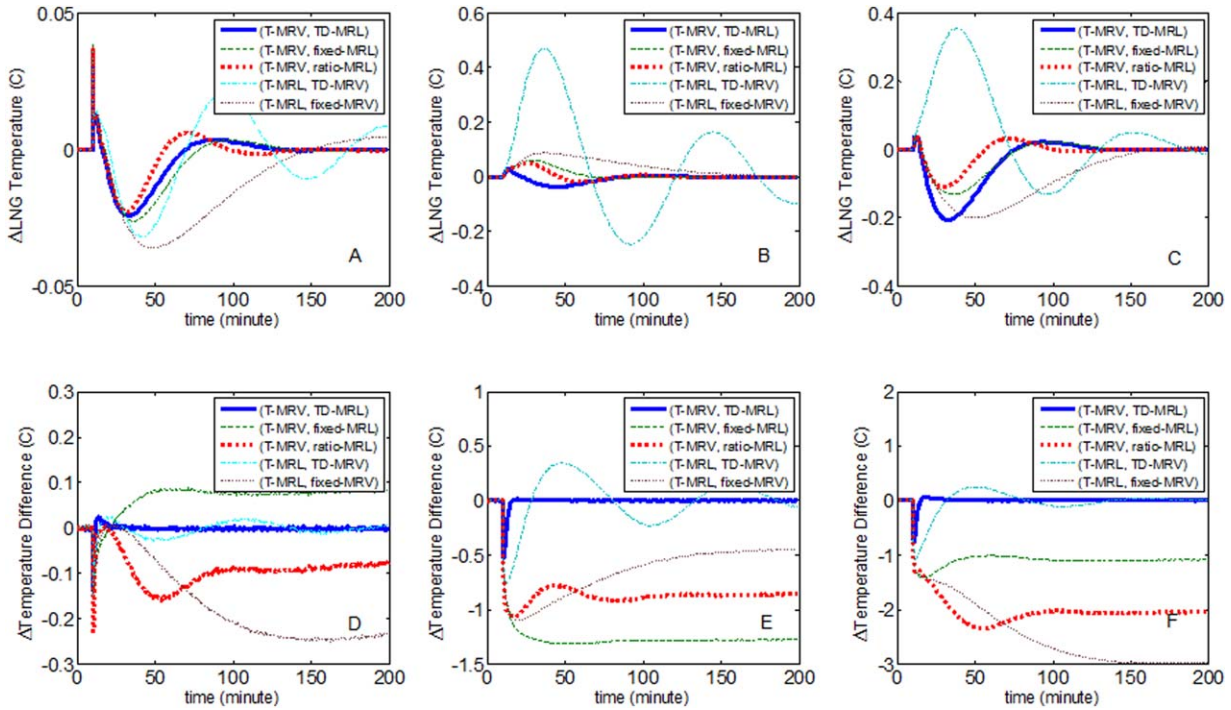

Figure 10. Responses of the controlled variables under a (MRV, MRL) configuration after D1, D2, and D3.

[Color figure can be viewed in the online issue, which is available at wileyonlinelibrary.com.]

Table 4. IAE Values of the Various Structures after Disturbances

	LNG Temperature (T)			Temperature Difference (TD)		
Structure	D1	D2	D3	D1	D2	D3
Fixed LNG Production						
(T-MRV, TD-MRL)	0.937	1.674	8.108	0.6097	1.668	2.903
(T-MRV, fixed-MRL)	1.122	2.114	5.945			
(T-MRV, ratio-MRL)	0.809	1.759	4.004			
(T-MRL, TD-MRV)	2.915	40.017	30.838	2.565	41.235	47.45
(T-MRL, fixed-MRV)	2.759	7.053	15.640			
Floating LNG Production						
(T-NG, TD-MRV, fixed-MRL)	0.556	4.879	3.799	1.585	16.379	21.202
(T-NG, TD-MRL, fixed-MRV)	0.434	0.780	3.356	0.602	1.644	2.594
(T-MRV, TD-NG, fixed-MRL)	0.621	8.683	12.515	1.448	12.139	16.985
(T-MRL, TD-NG, fixed-MRV)	1.750	5.692	6.442	17.447	41.521	219.870
(T-NG, TD-MRL, ratio-MRV)	0.485	3.049	7.077	0.592	2.206	3.555
(T-NG, TD-MRL, LNG-MRV)	0.518	0.804	3.610	0.562	1.659	2.772

case, whereas the (NG, MRV) and (NG, MRL) configurations correspond to the floating production case. In this study, all control loops were initially tuned using the autotuning facility in Hysys™, and finely tuned by trial and error to obtain the best resulting responses against the disturbances. All control loops including LNG temperature and every possible optimizing controller are configured using a cascade structure.

Fixed LNG production case

Various control schemes from the (MRV, MRL) configuration shown in Figure 9 were evaluated. Figure 10 shows the closed-loop responses for the main disturbances. The (T-MRV, TD-MRL) structure showed satisfactory performance in rejecting disturbances, as was expected from interaction analysis. In Figure 10, the TD responses appears to be nicely decoupled from the T response, as predicted from its dynamic features with a large difference in response speed, as shown in Figure 6. The TD quickly compensated for every type of disturbance with little effect on the LNG temperature loop. These results show that the TD control loop to maximize both the process efficiency and operation safety can be included into cryogenic exchanger control with little loss of transient control performance in the whole control system. The (T-MRL, TD-MRV) structure gave poor responses with a large oscillation and settling time for every type of disturbance. The poor performance of this pairing is mainly due to the insensitivity of each controlled variable on changes to its respective manipulated variable, which is also reflected from its RGA magnitude.

The other possible structures in the (MRV, MRL) configuration were also tested to observe the relative performance of the (T-MRV, TD-MRL) structure more clearly. In these structures, the loop (TD-MRL) is replaced with another loop for (1) controlling the MRL flow constant (T-MRV, fixed-MRL) or (2) controlling MRL/MRV ratio by adjusting the MRL flow (T-MRV, ratio-MRL). The MRL/MRV ratio can be used as an auxiliary control loop to maintain the composition of refrigerants entering the precooling and subcooling bundle over the operating map.[17] The (T-MRL, fixed-MRV) scheme was also evaluated as an alternative of the (T-MRV, fixed-MRL) scheme.

Figure 10 and Table 4 show that the LNG temperature control performance of the (T-MRV, TD-MRL), (T-MRV,

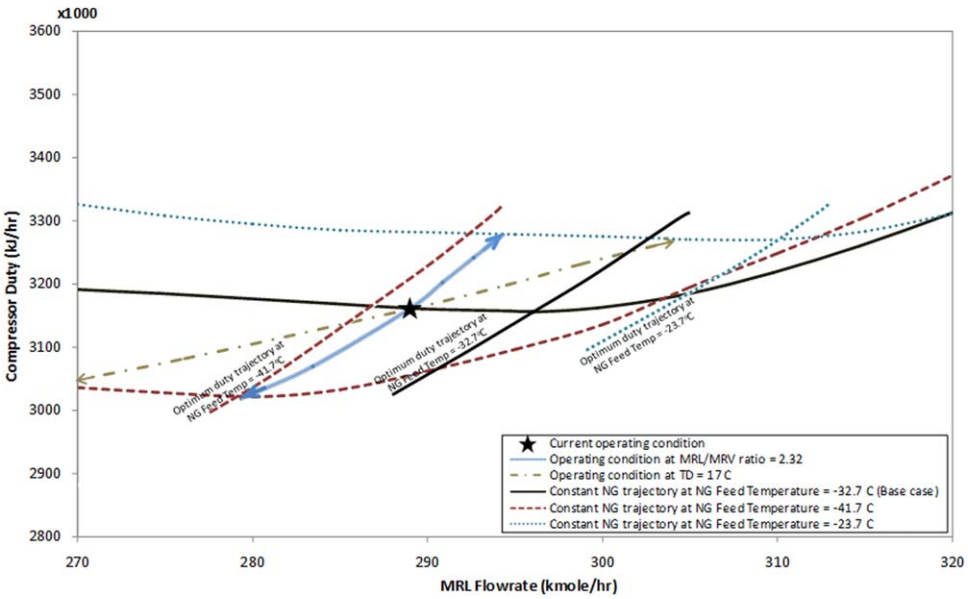

Figure 11. Projection of the operating conditions at a constant TD and MRL/MRV ratio at different NG feed temperatures.

[Color figure can be viewed in the online issue, which is available at wileyonlinelibrary.com.]

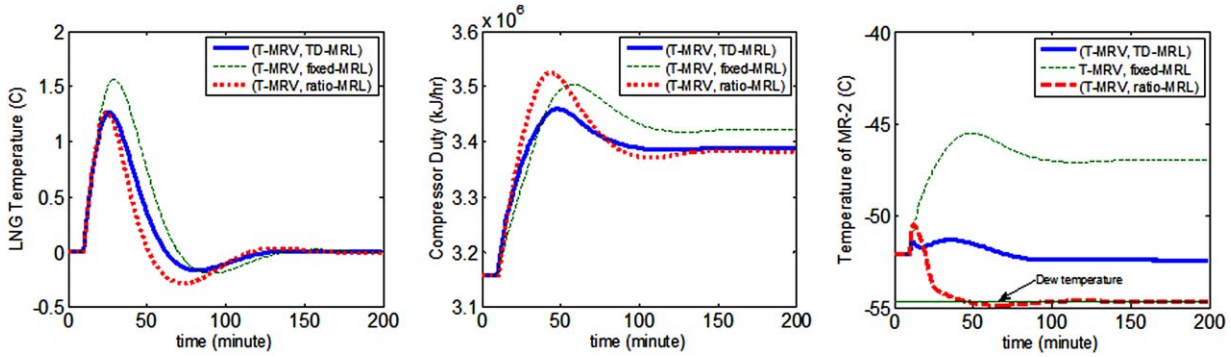

Figure 12. Responses of the process variables after ramping up the LNG flow rate by 5% under a (MRV, MRL) configuration and its derivatives.

[Color figure can be viewed in the online issue, which is available at wileyonlinelibrary.com.]

fixed-MRL), and (T-MRV, ratio-MRL) structures differed according to the type of disturbance but were relatively good for all three structures. Conversely, as shown in Steady-State Optimality Behavior of the C_3MR Liquefaction Process section, the (T-MRV, fixed-MRL) and (T-MRV, ratio-MRL) structures likely move the operation either quickly further away from the optimum point or across to the infeasible region because the TD is not controlled and drifts away from a desirable target. Note that the (T-MRL, fixed-MRV) scheme showed poor performance in controlling the LNG temperature nevertheless of single loop control without additional TD loop.

Figure 11 shows in more detail how the optimal operation lines are shifted according to changes in NG feed temperature. By maintaining the TD in the (T-MRV, TD-MRL) structure, the operating condition was always moving in the same direction as the optimum line for giving the minimum compressor duty, which allows the process to remain around a desirable operation point. Note that when the NG feed temperature is decreased to $-41.7°C$, the operating condition of the C_3MR process with the (T-MRV, ratio-MRL) structure was already located on the right side of the optimum duty trajectory, that is, on the infeasible operation region.

In the (MRV, MRL) configuration, the NG flow can be manipulated independently or varied by the factors associated with the upstream unit control and/or production planning, which will disturb the control of the liquefaction unit as a disturbance. The 5% step change in the NG flow rate was introduced to examine the effect of the LNG production rate variation on the control performance. Figure 12 shows the response of the LNG temperature, the resulting compressor duty and warm-end outlet MR stream temperature after increasing the NG flow rate. The (T-MRV, TD-MRL) structure still showed a fast and stable transient response with a low required compressor duty. The (T-MRV, ratio-MRL) structure also showed a reasonable transient low compressor duty similar to the (T-MRV, TD-MRL) structure. However, the operating point in the (T-MRV, ratio-MRL) structure moved to the infeasible region across its dew temperature. The (T-MRV, fixed-MRL) structure showed the worst transient response and highest duty.

Floating LNG production case

In the floating LNG production case, the control structures were derived from the (NG, MRV) and (NG, MRL) configurations. Therefore, either the MRL or the MRV flow rate will be a free manipulated variable to be either fixed or used for other control tasks. Figure 13 shows the four basic control structures in the floating production case, where the free manipulated variable, MRL or MRV, was flow controlled. Figure 14 presents the closed-loop responses of the four basic control structures for feed disturbances. As shown in

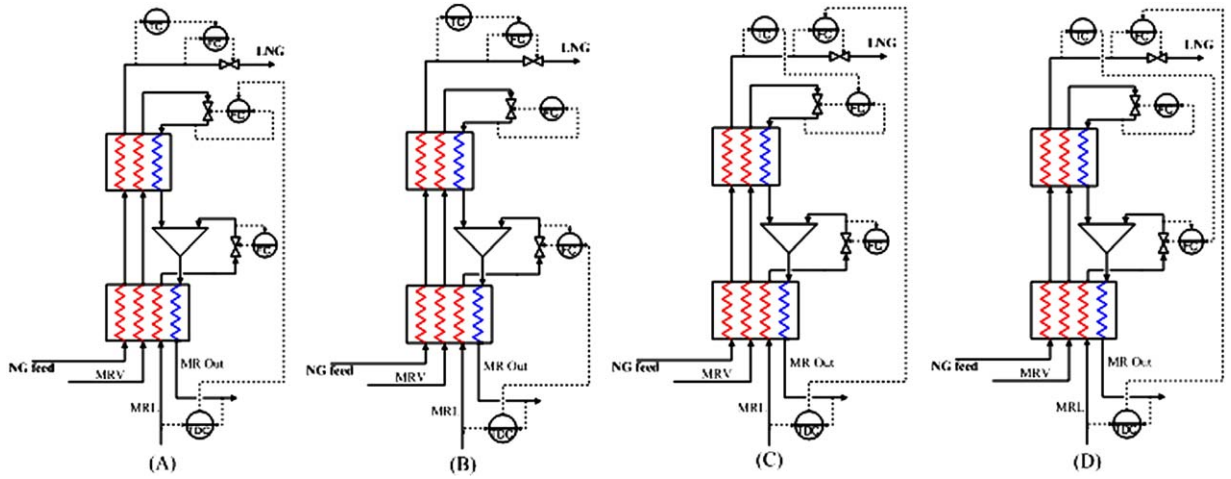

Figure 13. Basic control structures in the floating LNG case, (A) (T-NG, TD-MRV, fixed-MRL), (B) (T-NG, TD-MRL, fixed-MRV), (C) (T-MRV, TD-NG, fixed-MRL), and (D) (T-MRL, TD-NG, fixed-MRV).

[Color figure can be viewed in the online issue, which is available at wileyonlinelibrary.com.]

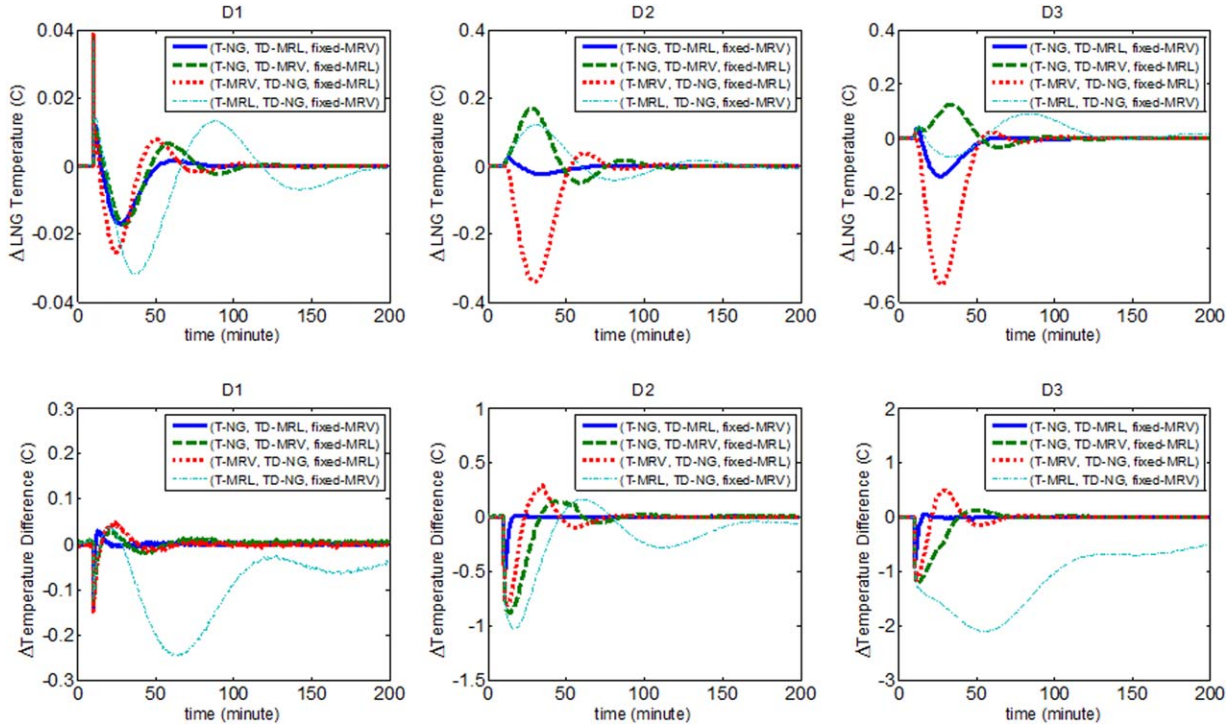

Figure 14. Responses of the controlled variables in the basic control structures of floating LNG case after D1, D2, and D3.

[Color figure can be viewed in the online issue, which is available at wileyonlinelibrary.com.]

the figure, the (T-NG, TD-MRL) scheme showed the best performance with the most stable and rapid responses. Note that the TD returns quickly to its set point against feed disturbances with little loss of LNG temperature control. This suggests that a TD control loop to maximize the energy efficiency and operation safety can be introduced successfully without harming the basic control task, that is, maintaining the LNG temperature. The (T-MRV, TD-NG) structure also showed reasonably good performance but slightly poorer performance than the (T-NG, TD-MRV) scheme. In contrast,

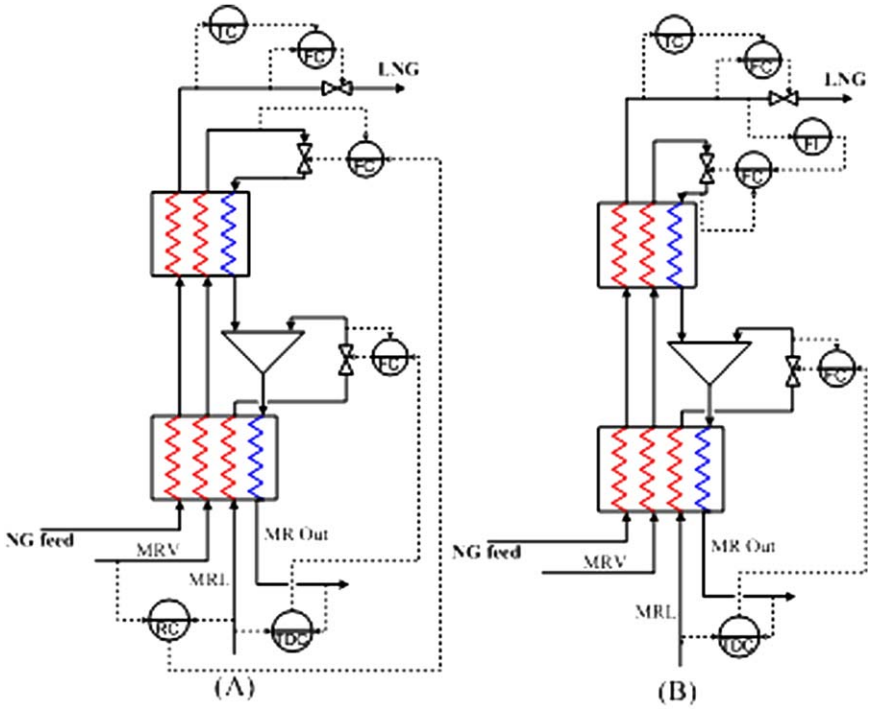

Figure 15. Derivatives structures for (NG, MRV, MRL) configuration, (A) (T-NG, TD-MRL, ratio-MRV) and (B) (T-NG, TD-MRL, LNG-MRV).

[Color figure can be viewed in the online issue, which is available at wileyonlinelibrary.com.]

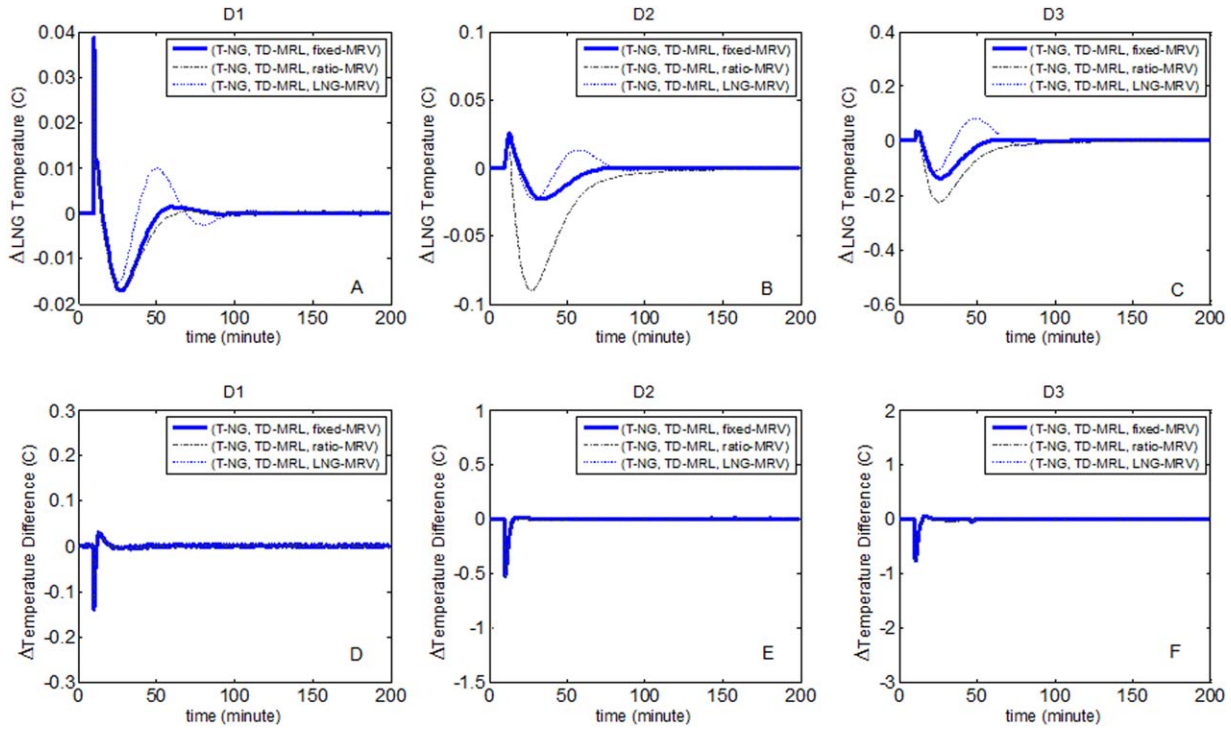

Figure 16. Performance of the (NG, MRV, MRL) configuration and its derivatives.

[Color figure can be viewed in the online issue, which is available at wileyonlinelibrary.com.]

RGA interaction indices strongly recommended the (T-MRV, TD-NG) scheme. Conversely, both (T-NG, TD-MRV) and (T-MRV, TD-NG) structures showed poorer responses with a larger overshoot and slower responses than the (T-NG, TD-MRL) structure. The (T-MRL, TD-NG) scheme with negative and close to zero RGA elements showed the poorest performance.

The free manipulated variable MRV in the (T-NG, TD-MRL) structure can be used in two ways: as a control element for (1) the MRV/MRL flow ratio and (2) for a LNG production target. Connecting the LNG flow rate to the MRV will create a supervisory control loop that is assigned to maintain a certain desired LNG production level in the long term. Whenever the LNG flow rate is varied as a result of controller action to maintain the LNG temperature, the MRV flow rate will be adjusted accordingly to return the LNG flow rate to its desired level. Figure 15 shows the arrangements of the two approaches. Figure 16 compares the closed-loop responses of the three different (T-NG, TD-MRL) schemes. The basic (T-NG, TD-MRL, fixed-MRV) scheme still showed better performance than other two (T-NG, TD-MRL) derivatives. The (T-NG, TD-MRL, LNG-MRV) scheme was the next best structure.

Conclusions

Possible control structures and steady-state optimality behavior of C_3MR process were studied thoroughly to determine the best control strategies for energy optimizing control. Steady-state optimality analysis showed that the TD between the warm-end inlet and outlet MR streams is the correct additional control variable for achieving an energy efficient and safe operation of the C_3MR liquefaction process. In addition, the optimum for giving a minimum compressor duty occurs at the dew temperature of the warm-end outlet MR stream (MR-2). By following a constant TD line, the process can always be kept close to the optimum operating point remaining within a feasible region while securing a constant safety margin. Conversely, control structures using other variables, such as constant MRL flow rate, MRV flow rate, and MRL/MRV ratio, will likely drift the liquefaction process away from the optimum point or cross the dew point line to reach an infeasible region. The steady-state optimality map developed in this study is expected to contribute useful insights about the behavior of the respective process. Further, the approach is not limited only for the C_3MR process but also for other NG liquefaction processes.

Six possible basic control structures and their derivatives were investigated fully through interaction analyses and dynamic response evaluations. As a result, in the fixed LNG production case, the (T-MRV, TD-MRL) scheme showed the best performance with the most stable and fastest disturbance compensation. In the floating LNG production case, the (T-NG, TD-MRL, fixed-MRV) scheme was found to be the best structure. In both two cases, the TD quickly returned to its set point against feed disturbances with little loss of control performance of the LNG temperature. This suggests that the TD control loop can be introduced successfully into the C_3MR process to maximize the energy efficiency and operation safety with little loss of the basic control task, that is, controlling the LNG temperature.

Using the free manipulated variable in the floating case, that is, (T-NG, TD-MRL, ratio-MRV) and (T-NG, TD-MRL, LNG-MRV), did not add a significant benefit to the performance of LNG temperature and TD loop. However, the (T-NG, TD-MRL, LNG-MRV) can still be implemented if maintaining LNG production rate is deemed necessary in long term.

Acknowledgment

This research was supported by a grant from the Gas Plant R&D Center funded by the Ministry of Land, Transportation, and Maritime Affairs (MLTM) of the Korean government

Literature Cited

1. Harrold D. Design a turnkey floating LNG facility. *Hydrocarbon Process*. 2004;83:47–51.
2. Pillarella M, Liu YN, Petrowski J, Bower R. The C3MR liquefaction cycle: versatility for a fast growing, ever changing LNG industry. *The 15th International Conference on LNG*. Barcelona, Spain, 2007.
3. Hatcher P, Khalilpour R, Abbas A. Optimisation of LNG mixed-refrigerant process considering operation and design objectives. *Comput Chem Eng*. 2012;41:123–133.
4. Wang M, Zhang J, Xu Q. Optimal design and operation of a C_3MR refrigeration system for natural gas liquefaction. *Comput Chem Eng*. 2012;39:84–95.
5. Helgestad DE. Modeling and optimization of the C3MR process for liquefaction of natural gas, in Process Systems Engineering 2009, Norwegian University of Science and Technology, NTNU: Trondheim, Norway.
6. Lee GC, Smith R, Zhu XX. Optimal synthesis of mixed-refrigerant systems for low-temperature processes. *Ind Eng Chem Res*. 2002;41:5016–5028.
7. Nogal FD, Kim J, Perry S, Smith R. Optimal design of mixed refrigerant cycles. *Ind Eng Chem Res*. 2008;47:8724–8740.
8. Khan MS, Lee S, Lee M. Optimization of single mixed refrigerant natural gas liquefaction plant with nonlinear programming. *Asia-Pac J Chem Eng*. 2012;7:62–70.
9. Yuli AH, Yeo GC, Lee M. Plant-wide control for the economic operation of modified single mixed refrigerant process for an offshore natural gas liquefaction plant. *Chem Eng Res Des*. In press. DOI: 10.1016/j.cherd.2013.11.009.
10. Skogestad S. Control structure design for complete chemical plants. *Comput Chem Eng*. 2004;28:219–234.
11. Jensen JB, Skogestad S. Steady-state operational degrees of freedom with application to refrigeration cycles. *Ind Eng Chem Res*. 2009;48:6652–6659.
12. Venkatarathnam G. *Cryogenic Mixed Refrigerant Process*. NY: Springer, 2008.
13. Shinskey FG. *Energy Conservation through Control*. London: Academic Press Inc., 1978.
14. Aspelund A, Gundersen T, Myklebust J, Nowak MP, Tomasgard A. An optimization-simulation model for a simple LNG process. *Comput Chem Eng*. 2010;34:1606–1617.
15. Morud J, Skogestad S. Dynamic behaviour of integrated plants. *J Process Control*. 1996;6:145–156.
16. McAvoy TJ. Some results on dynamic interaction analysis of complex control systems. *Ind Eng Process Des Dev*. 1983;22:42–49.
17. Mandler JA, Brochu PA, Fotopoulos J. New Control Strategies for the LNG Process. *Proceedings of the LNG 12 Conference*. Perth, W. A., 1998:C.3-1–C.3–11.

Manuscript received May 8, 2013, and revision received Nov. 30, 2013.